

Selective Convolutional Descriptor Aggregation for Fine-Grained Image Retrieval

Xiu-Shen Wei, Jian-Hao Luo, and Jianxin Wu

National Key Laboratory for Novel Software Technology, Nanjing University,
Nanjing, China, 210023

Abstract Deep convolutional models pre-trained for the ImageNet classification task have been successfully adopted to tasks in other domains, such as texture description and object proposal generation, but these tasks require annotations for images in the new domain. In this paper, we focus on a novel and challenging task in the pure unsupervised setting: fine-grained image retrieval. Even with image labels, fine-grained images are difficult to classify, let alone the unsupervised retrieval task. We propose the Selective Convolutional Descriptor Aggregation (SCDA) method. SCDA firstly localizes the main object(s) in fine-grained images, a step that discards noisy background and keeps useful deep descriptors. The selected descriptors are then aggregated and dimensionality reduced into a short feature vector using the best practices we found. SCDA is unsupervised, using no image label or bounding box annotation. Experiments on four fine-grained datasets confirm the effectiveness of SCDA. Visualization of the SCDA features shows that they correspond to visual attributes (even subtle ones), which might explain SCDA’s high accuracy in fine-grained retrieval.

Keywords: Fine-grained image retrieval, selection and aggregation, unsupervised object localization.

1 Introduction

After the breakthrough in image classification using Convolutional Neural Networks (CNN) [1], pre-trained CNN models trained for one task (e.g., recognition or detection) have also been applied to domains different from their original purposes (e.g., for describing texture [2] or finding object proposals [3]). Such adaptations of pre-trained CNN models, however, still require further annotations in the new domain (e.g., image labels). In this paper, we show that for fine-grained images which contain only subtle differences among categories (e.g., varieties of dogs), pre-trained CNN models can both localize the main object and find images in the same variety. Since no supervision is used, we call this novel and challenging task *fine-grained image retrieval*.

In fine-grained image classification [4–9], categories correspond to varieties in the same species. The categories are all similar to each other, only distinguished by slight and subtle differences. Therefore, an accurate system usually requires

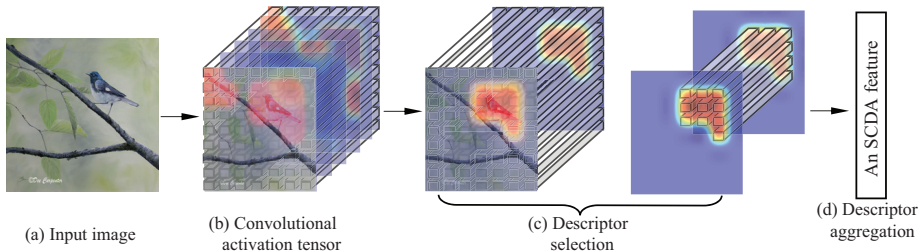


Figure 1. Pipeline of the proposed SCDA method. (Best viewed in color.)

strong annotations, e.g., bounding boxes for object or even object parts. Such annotations are expensive and unrealistic in many real applications. In answer to this difficulty, there are attempts to categorize fine-grained images with only image-level labels, e.g., [6–9].

In this paper, we handle a more challenging but more realistic task, i.e., Fine-Grained Image Retrieval (FGIR). In FGIR, given database images of the same species (e.g., birds, flowers or dogs) and a query, we should return images which are in the same variety as the query, without resorting to any other supervision signal. FGIR is useful in applications such as biological research and bio-diversity protection. FGIR is also different from and difficult than general-purpose image retrieval. Objects in fine-grained images have only subtle differences, and vary in poses, scales and rotations.

To meet these challenges, we propose the Selective Convolutional Descriptor Aggregation (SCDA) method, which automatically localizes the main object in fine-grained images and extracts discriminative representations for them. In SCDA, only a pre-trained CNN model (from ImageNet which is not fine-grained) is used and we use absolutely no supervision. As shown in Fig. 1, the pre-trained CNN model first extracts convolution activations for an input image. We propose a novel approach to determine which part of the activations are useful (i.e., to localize the object). These useful descriptors are then aggregated and dimensionality reduced to form a vector representation using practices we propose in SCDA. Finally, a nearest neighbor search ends the FGIR process.

We conducted extensive experiments on four popular fine-grained datasets, i.e., *CUB200-2011* [10], *Stanford Dogs* [11], *Oxford Flowers 102* [12] and *Oxford-IIIT Pets* [13] for image retrieval. In addition, we also report the classification accuracy of the SCDA method, which only uses the image labels. Both retrieval and classification experiments verify the effectiveness of SCDA. The key advantages and major contributions of our method are:

1. We propose a simple yet effective approach to localize the main object. This localization is unsupervised, without utilizing bounding boxes, image labels, object proposals, or additional learning. SCDA selects only useful deep descriptors and removes background or noise, which benefits the retrieval task. For example, SCDA’s retrieval mAP on *Oxford Flowers* is 77.56%, significantly higher than the baseline without descriptor selection (70.73%). With

the ensemble of multiple CNN layers and the proposed dimensionality reduction practice, SCDA has shorter but more accurate representation than existing deep learning based methods (cf. Sec. 4).

2. As shown in Fig. 8, the compressed SCDA feature has stronger correspondence to visual attributes (even subtle ones) than the deep activations, which might explain the success of SCDA for fine-grained tasks.

2 Related Works

We will first briefly review two lines of related works: deep learning approaches for image retrieval and research on fine-grained images.

2.1 Deep Learning for Image Retrieval

Until recently, most image retrieval approaches were based on local features (typically SIFT) and feature aggregation strategies (e.g., VLAD [14] and FV [15]). After the success of CNN [1], image retrieval also embraced deep learning. Out-of-the-box features from pre-trained deep networks were shown to achieve state-of-the-art results in many vision related tasks, including image retrieval [16].

Very recently, some efforts (e.g., [17–21]) studied what deep descriptors can be used and how to use them in image retrieval, and achieved satisfactory results. However, these approaches were all designed for general image retrieval, which is quite different from fine-grained image retrieval. As will be shown by our experiments, state-of-the-art general image retrieval approaches do not work well for FGIR.

2.2 Fine-Grained Image Tasks

Fine-grained classification has been popular in the past few years [4–9]. Because it is not realistic to obtain strong annotations (object bounding boxes and part annotations) for large amount of images, more algorithms attempted to classify fine-grained images using only image-level labels, e.g., [6–9].

Few work have touched unsupervised retrieval of fine-grained images. Wang et al. [22] proposed Deep Ranking to learn similarity between fine-grained images. However, it requires image-level labels to build a set of triplets, which is not unsupervised and cannot scale well.

The most related research to FGIR is [23]. The authors of [23] proposed the fine-grained image *search* problem. [23] used the bag-of-word model with SIFT features, while we use pre-trained CNN models. Beyond this difference, a more important difference is how the database is constructed.

[23] constructed a hierarchical database by merging several existing image retrieval datasets, including fine-grained ones (e.g., *CUB200-2011* and *Stanford Dogs*) and general image retrieval datasets (e.g., *Oxford Buildings* and *Paris*). Given a query, [23] first determines its meta class, and then does fine-grained image search if the query belongs to the fine-grained meta category. In FGIR,

the database contains images of one single species, which is more suitable in fine-grained applications. For example, a bird protection project may not want to find dog images given a bird query. To our best knowledge, this is *the first attempt to fine-grained image retrieval using deep learning*.

3 Selective Convolutional Descriptor Aggregation

In this paper, we follow the notations in [24]. The term “feature map” indicates the convolution results of one channel; the term “activations” indicates feature maps of all channels in a convolution layer; and the term “descriptor” indicates the d -dimensional component vector of activations. “pool₅” refers to the activations of the max-pooled last convolution layer, and “fc₈” refers to the activations of the last fully connected layer.

Given an input image I of size $H \times W$, the activations of a convolution layer are formulated as an order-3 tensor T with $h \times w \times d$ elements, which include a set of 2-D feature maps $S = \{S_n\}$ ($n = 1, \dots, d$). S_n of size $h \times w$ is the n th feature map of the corresponding channel. From another point of view, T can be also considered as having $h \times w$ cells and each cell contains one d -dimensional deep descriptor. We denote the deep descriptors as $X = \{\mathbf{x}_{(i,j)}\}$, where (i, j) is a particular cell ($i \in \{1, \dots, h\}, j \in \{1, \dots, w\}, \mathbf{x}_{(i,j)} \in \mathcal{R}^d$). For instance, by employing the popular pre-trained VGG-16 model [25] to extract deep descriptors, we can get a $7 \times 7 \times 512$ activation tensor in pool₅ if the input image is 224×224 . Thus, on one hand, for this image, we have 512 feature maps (i.e., S_n) of size 7×7 ; on the other hand, 49 deep descriptors of 512-d are also obtained.

3.1 Selecting Convolutional Descriptors

What distinguishes SCDA from existing deep learning-based image retrieval methods is: using only the pre-trained model, SCDA is able to find *useful deep convolutional features*, which in effect *localizes the main object* in the image and discards irrelevant and noisy image regions. Note that the pre-trained model is *not* fine-tuned using the target fine-grained dataset. In the following, we propose our descriptor selection method, and then present quantitative and qualitative localization results.

Descriptor Selection After obtaining the pool₅ activations, the input image I is represented by an order-3 tensor T , which is a sparse and *distributed* representation [26, 27].¹ In Fig. 2, we show four images taken from two fine-grained

¹ The distributed representation argument claims that concepts are encoded by a distributed pattern of activities spread across multiple neurons [28]. In deep neural networks, a distributed representation means a many-to-many relationship between two types of representations (i.e., concepts and neurons): Each concept is represented by a pattern of activity distributed over many neurons, and each neuron participates in the representation of many concepts [26, 27].

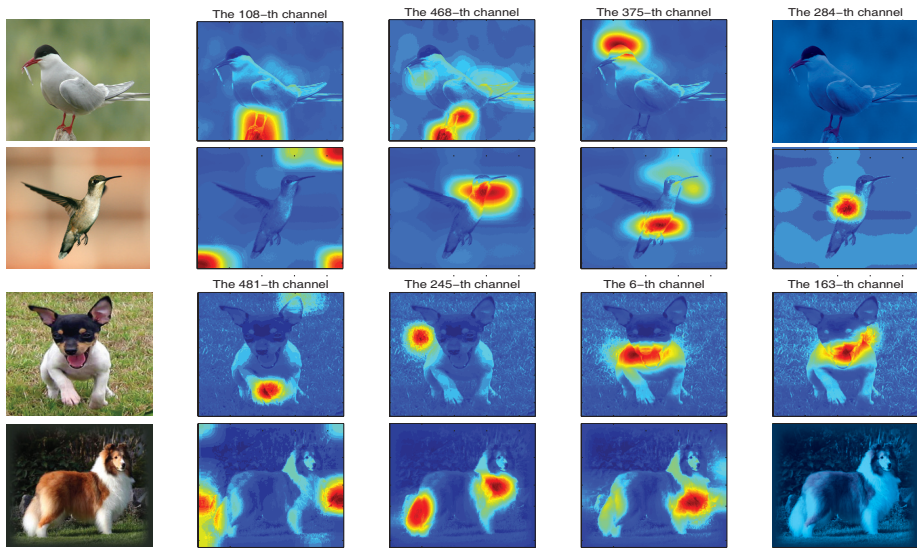


Figure 2. Sampled feature maps of four fine-grained images. Although we resize the images for better visualization, our method can deal with images of any resolution. (The figure is best viewed in color.)

datasets, *CUB200-2011* [10] and *Stanford Dogs* [11]. We randomly sample several feature maps from the 512 feature maps in pool_5 and overlay them to original images for better visualization. As can be seen from Fig. 2, the activated regions of the sampled feature map (highlighted in warm color) may indicate semantically meaningful parts of birds or dogs, but can also indicate some background or noisy parts in these fine-grained images.

In addition, the semantic meanings of the activated regions are quite different even for the same channel. For example, in the 468th feature map for *birds*, the activated region in the first image indicates the *Artic tern*’s claws and the second does the *hummingbird*’s head. In the 163th feature map for *dogs*, the first indicates the *toy terrier*’s mouth, while the second even has no activated region for the *Shetland sheepdog*. More examples can be found in the supplementary material. In addition, there are also some activated regions representing the background, e.g., the 108th feature map for *hummingbird* and the 481th one for *Shetland sheepdog*. Fig. 2 conveys that *not all deep descriptors are useful*, and *one single channel contains at best weak semantic information* due to the distributed nature of this representation. Therefore, selecting and using only useful deep descriptors (and removing noise) is necessary. However, in order to decide which deep descriptor is useful (i.e., containing the object we want to retrieve), we cannot count on any single channel individually.

We propose a simple yet effective method (shown in Fig. 4) whose quantitative and qualitative evaluation will be demonstrated in the next section. Although one single channel is not very useful, if many channels fire at the same

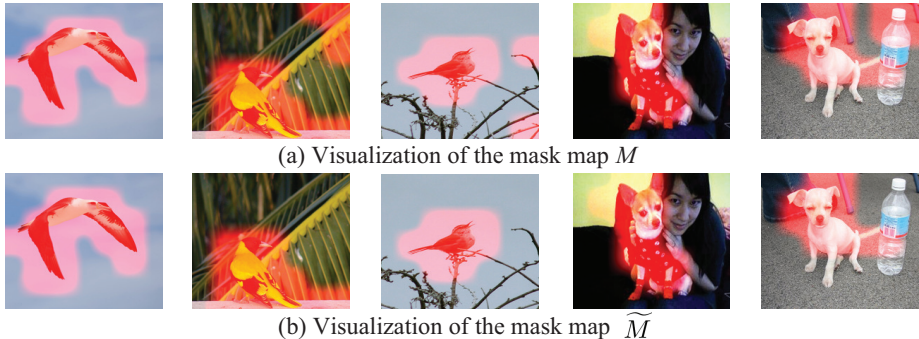


Figure 3. Visualization of the mask map M and the corresponding largest connected component \widetilde{M} . The selected regions are highlighted in red. (Best viewed in color.)

region, we could expect this region to be an object rather than the background. Therefore, in the proposed method, we add up the obtained pool_5 activation tensor through the depth direction. Thus, the $h \times w \times d$ 3-D tensor becomes an $h \times w$ 2-D tensor, which we call the “activation map”, i.e., $A = \sum_{n=1}^d S_n$ (where S_n is the n th feature map in pool_5). For the activation map A , there are $h \times w$ summed activation responses, corresponding to $h \times w$ positions. Based on the aforementioned observation, it is straightforward to say that the higher activation response a particular position (i, j) is, the more possibility of its corresponding region being part of the object. Then, we calculate the mean value \bar{a} of all the positions in A as the threshold to decide which positions localize objects: the position (i, j) whose activation response is higher than \bar{a} indicates the main object, e.g., birds or dogs, might appear in that position. A mask map M of the same size as A can be obtained as:

$$M_{i,j} = \begin{cases} 1 & \text{if } A_{i,j} > \bar{a} \\ 0 & \text{otherwise} \end{cases}, \quad (1)$$

where (i, j) is a particular position in these $h \times w$ positions.

The figures in the first row of Fig. 3 show some examples of the mask maps for birds and dogs. In these figures, we first resize the mask map M using the bicubic interpolation, such that its size is the same as the input image. We then overlay the corresponding mask map (highlighted in red) onto original images. Even though the proposed method does not train on these datasets, the main objects (birds or dogs) can be roughly detected. But, as can be seen from the 2nd, 3rd and 5th figure in the first row, there are still several small noisy parts activated on complicated background. Fortunately, because the noisy parts are usually smaller than the main object, we collect the largest connected component of M , which is denoted as \widetilde{M} , to get rid of the interference caused by noisy parts. In the second row, the main objects are kept by \widetilde{M} , while the noisy parts are discarded, e.g., the *plant* and the *water bottle*.

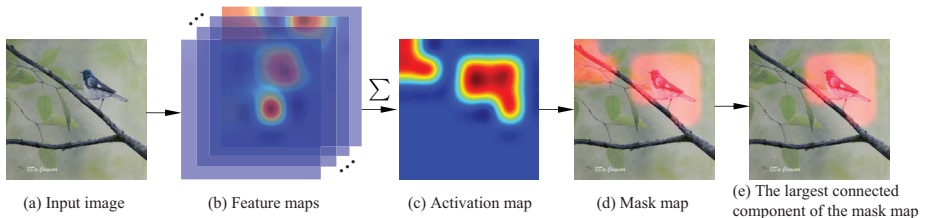


Figure 4. Selecting useful deep convolutional descriptors. (Best viewed in color.)

Therefore, we use \widetilde{M} to select useful and meaningful deep convolutional descriptors. The descriptor $\mathbf{x}_{(i,j)}$ should be kept when $\widetilde{M}_{i,j} = 1$, while $\widetilde{M}_{i,j} = 0$ means the position (i,j) might have background or noisy parts:

$$F = \left\{ \mathbf{x}_{(i,j)} \mid \widetilde{M}_{i,j} = 1 \right\}, \quad (2)$$

where F stands for the selected descriptor set, which will be aggregated into the final representation for retrieving fine-grained images. The whole convolutional descriptor selection process is illustrated in Fig. 4.

Qualitative Evaluation In this section, we give the qualitative evaluation of the proposed descriptor selection process. Because the two fine-grained datasets (i.e., *CUB200-2011* and *Stanford Dogs*) supply the ground-truth bounding box for each image, it is desirable to evaluate the proposed method for object localization. However, as seen in Fig. 3, the detected regions are irregular shaped. So, the minimum rectangle bounding boxes which contain the detected regions are returned as our object localization predictions. We evaluate the proposed method to localize the whole-object (birds or dogs) on their test sets. Example predictions can be seen in Fig. 5. From these figures, the predicted bounding boxes approximate the ground-truth ones, and even some results are better than the ground truth. For instance, in the second dog image shown in Fig. 5, the predicted bounding box can cover both dogs; and in the third one, the predicted box contains less background, which is beneficial to retrieval performance. However, since we utilize no supervision, some details of the fine-grained objects, e.g., birds’ tails, cannot be contained accurately by the predicted bounding boxes.

Quantitative Evaluation In addition, we also report the results in terms of the Percentage of Correctly Localized Parts (PCP) metric in Table 1. The reported metrics are the percentage of whole-object boxes that are correctly localized with a $>50\%$ IOU with the ground-truth bounding boxes. In this table, we also show the PCP results of two fine-grained parts (i.e., head and torso) reported in some previous part localization based fine-grained *classification* algorithms [4, 5, 29]. Because our method do not require any supervision, we can just compare the whole-object localization rates with that of fine-grained parts for a rough

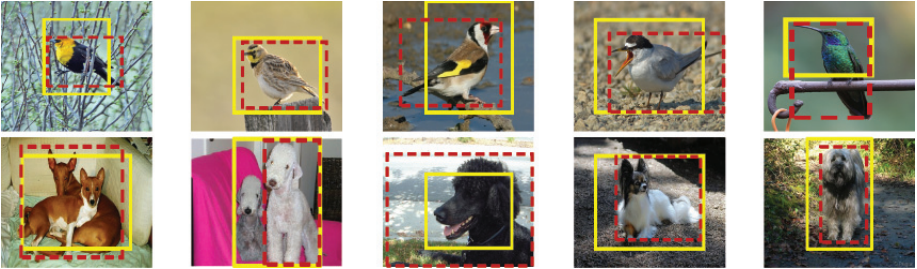


Figure 5. Samples of predicted object localization bounding box. The ground-truth bounding box is marked as the red dashed rectangle, while the predicted one is marked in the solid yellow rectangle. (The figure is best viewed in color.)

Table 1. Comparison of object localization performance on two fine-grained datasets.

Dataset	Method	Train phase		Test phase		Head	Torso	Whole-object
		BBox	Parts	BBox	Parts			
<i>CUB200-2011</i>	Strong DPM [29]	✓	✓	✓		43.49%	75.15%	N/A
	Part-based R-CNN with BBox [4]	✓	✓	✓		68.19%	79.82%	N/A
	Deep LAC [5]	✓	✓	✓		74.00%	96.00%	N/A
	Part-based R-CNN [4]	✓	✓			61.42%	70.68%	N/A
	Ours					N/A	N/A	76.79%
<i>Stanford Dogs</i>	Ours					N/A	N/A	78.86%

comparison. In fact, the *torso* bounding box is highly similar to that of the whole-object in *CUB200-2011*. By comparing the results of PCP for *torso* and our *whole-object*, we find that, even though our method is unsupervised, the localization performance is just slightly lower or even comparable to that of these algorithms using strong supervisions, e.g., ground-truth bounding box and parts annotations (even in the test phase).

3.2 Aggregating Convolutional Descriptors

After selecting $F = \left\{ \mathbf{x}_{(i,j)} \mid \widetilde{M}_{i,j} = 1 \right\}$, we compare several encoding or pooling approaches to aggregate these convolutional features, and then give our proposal.

- **VLAD** [14] uses k -means to find a codebook of K centroids $\{\mathbf{c}_1, \dots, \mathbf{c}_K\}$ and maps $\mathbf{x}_{(i,j)}$ into a single vector $\mathbf{v}_{(i,j)} = [\mathbf{0} \dots \mathbf{0} \ \mathbf{x}_{(i,j)} - \mathbf{c}_k \dots \mathbf{0}] \in \mathcal{R}^{K \times d}$, where \mathbf{c}_k is the closest centroid to $\mathbf{x}_{(i,j)}$. The final representation is $\sum_{i,j} \mathbf{v}_{(i,j)}$.
- **Fisher Vector** [15]: FV is similar to VLAD, but uses a soft assignment (i.e., Gaussian Mixture Model) instead of using k -means. Moreover, FV also includes second-order statistics.²

² For parameter choice of VLAD/FV, we follow the suggestions reported in [30]. The number of clusters in VLAD and the number of Gaussian components in FV are both set to 2. Larger values lead to lower accuracy.

Table 2. Comparison of different encoding or pooling approaches for FGIR.

Approach	Dimension	<i>CUB200-2011</i>		<i>Stanford Dogs</i>	
		top1	top5	top1	top5
VLAD	1,024	55.92%	62.51%	69.28%	74.43%
Fisher Vector	2,048	52.04%	59.19%	68.37%	73.74%
avgPool	512	56.42%	63.14%	73.76%	78.47%
maxPool	512	58.35%	64.18%	70.37%	75.59%
avg&maxPool	1,024	59.72%	65.79%	74.86%	79.24%

- **Pooling approaches.** We also try two traditional pooling approaches, i.e., max-pooling and average-pooling, to aggregate the deep descriptors.

After encoding or pooling into a single vector, for VLAD and FV, the square root normalization and ℓ_2 -normalization are followed; for max- and average-pooling methods, we just do ℓ_2 -normalization (the square root normalization did not work well). Finally, the cosine similarity is used for nearest neighbor search. We use two datasets to demonstrate which type of aggregation method is optimal for fine-grained image retrieval. The original training and testing splits provided in the datasets are used. Each image in the testing set is treated as a query, and the training images are regarded as the gallery. The top- k mAP retrieval performance is reported in Table 2. We find the simpler aggregation methods such as max- and average-pooling achieve better retrieval performance comparing with the high-dimensional encoding approaches. These observations are also consistent with the findings in [20] for general image retrieval. We propose to concatenate the max-pooling and average-pooling representations, “avg&maxPool”, as our aggregation scheme. Its performance is significantly and consistently higher than the others. We use the “avg&maxPool” aggregation as “*SCDA feature*” to represent the whole fine-grained image.

3.3 Multiple Layer Ensemble

As studied in [31,32], the ensemble of multiple layers boost the final performance. Thus, we also incorporate another SCDA feature produced from the $\text{relu}_{5,2}$ layer which is three layers in front of pool_5 in the VGG-16 model [25].

Following pool_5 , we get the mask map $M_{\text{relu}_{5,2}}$ from $\text{relu}_{5,2}$. Its activations are less related to the semantic meaning than those of pool_5 . As shown in Fig. 6 (c), there are many noisy parts. However, the bird is more accurately detected than pool_5 . Therefore, we combine $\widetilde{M}_{\text{pool}_5}$ and $M_{\text{relu}_{5,2}}$ together to get the final mask map of $\text{relu}_{5,2}$. $\widetilde{M}_{\text{pool}_5}$ is firstly upsampled to the size of $M_{\text{relu}_{5,2}}$. We keep the descriptors when their position in both $\widetilde{M}_{\text{pool}_5}$ and $M_{\text{relu}_{5,2}}$ are 1, which are the final selected $\text{relu}_{5,2}$ descriptors. The aggregation process remains the same. Finally, we concatenate the SCDA features of $\text{relu}_{5,2}$ and pool_5 into a single representation, denoted by “SCDA⁺”:

$$\text{SCDA}^+ \leftarrow [\text{SCDA}_{\text{pool}_5}, \alpha \times \text{SCDA}_{\text{relu}_{5,2}}], \quad (3)$$

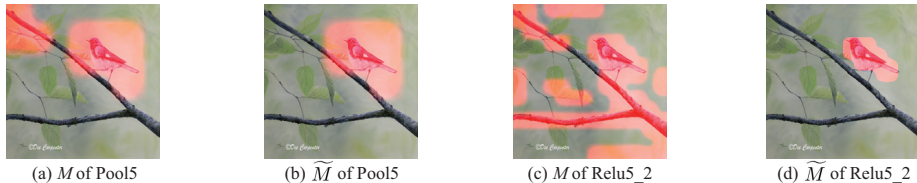


Figure 6. The mask map and its corresponding largest connected component of different CNN layers. (The figure is best viewed in color.)

where α is the coefficient for $\text{SCDA}_{\text{relu}_{5,2}}$. It is set to 0.5 for FGIR. The ℓ_2 normalization is followed. In addition, another SCDA^+ of the horizontal flip of the original image is incorporated, which is denoted as “ $\text{SCDA}_{\text{flip}}^+$ ” (4,096-d).

4 Experiments and Results

In this section, we report the fine-grained image retrieval results. In addition, as another evidence to prove the effectiveness of SCDA, we also report the fine-grained classification accuracy by fine-tuning the pre-trained model with image-level labels. In the experiments, we evaluate the proposed method on four benchmark fine-grained datasets, *CUB200-2011* [10] (200 classes, 11,788 images), *Stanford Dogs* [11] (120 classes, 20,580 images), *Oxford Flowers 102* [12] (102 classes, 8,189 images) and *Oxford-IIIT Pets* [13] (37 classes, 7,349 images). For the pre-trained deep model, the publicly available VGG-16 model [25] is employed to extract deep convolutional descriptors in MatConvNet [33].

4.1 Fine-Grained Image Retrieval Performance

We compare the proposed method with several baseline approaches and two state-of-the-art general image retrieval approaches, *SPoC* [20] and *CroW* [21]. The top-1 and top-5 mAP results are reported in Table 3.

For the fc_8 baseline, because it requires the input images at a fixed size, the original images are resized to 224×224 and then fed into VGG-16. In addition, we also feed the ground truth bounding boxes to replace the whole images. As shown in Table 3, because the ground truth bounding boxes of these fine-grained images just contain the main objects, the fc_8 feature of the ground truth bounding box achieves better performance than that of the whole images. Moreover, the retrieval results of the fc_8 feature using the bounding boxes predicted by our method are also shown in Table 3, which are slightly lower than the ground-truth ones. This observation validates the effectiveness of our method’s object localization once again.

For the pool_5 baseline, the pool_5 descriptors are extracted directly without any selection process. We pool them by both average- and max-pooling, and concatenate them into a 1,024-d representation. As shown in Table 3, the performance of pool_5 is better than “ fc_8_{im} ”, but much worse than the proposed SCDA

Table 3. Comparison of fine-grained image retrieval performance.

Method	Dimension	<i>CUB200-2011</i>		<i>Stanford Dogs</i>		<i>Oxford Flowers</i>		<i>Oxford Pets</i>	
		top1	top5	top1	top5	top1	top5	top1	top5
fc8_im	4,096	39.90%	48.10%	66.51%	72.69%	55.37%	60.37%	82.26%	86.02%
fc8_gtBBox	4,096	47.55%	55.34%	70.41%	76.61%	–	–	–	–
fc8_predBBox	4,096	45.24%	53.05%	68.78%	74.09%	57.16%	62.24%	85.55%	88.47%
Pool ₅	1,024	57.54%	63.66%	69.98%	75.55%	70.73%	74.05%	85.09%	87.74%
selectFV	2,048	52.04%	59.19%	68.37%	73.74%	70.47%	73.60%	85.04%	87.09%
selectVLAD	1,024	55.92%	62.51%	69.28%	74.43%	73.62%	76.86%	85.50%	87.94%
SPoC (w/o cen.)	256	34.79%	42.54%	48.80%	55.95%	71.36%	74.55%	60.86%	67.78%
SPoC (with cen.)	256	39.61%	47.30%	48.39%	55.69%	65.86%	70.05%	64.05%	71.22%
CroW	256	53.45%	59.69%	62.18%	68.33%	73.67%	76.16%	76.34%	80.10%
SCDA	1,024	59.72%	65.79%	74.86%	79.24%	75.13%	77.70%	87.63%	89.26%
SCDA ⁺	2,048	59.68%	65.83%	74.15%	78.54%	75.98%	78.49%	87.99%	89.49%
SCDA_flip ⁺	4,096	60.65%	66.75%	74.95%	79.27%	77.56%	79.77%	88.19%	89.65%

Table 4. Comparison of different compression methods on “SCDA_flip⁺”.

Method	Dimension	<i>CUB200-2011</i>		<i>Stanford Dogs</i>		<i>Oxford Flowers</i>		<i>Oxford Pets</i>	
		top1	top5	top1	top5	top1	top5	top1	top5
PCA	256	60.48%	66.55%	74.63%	79.09%	76.38%	79.32%	87.82%	89.75%
	512	60.37%	66.78%	74.76%	79.27%	77.15%	79.50%	87.46%	89.71%
SVD	256	60.34%	66.57%	74.79%	79.27%	76.79%	79.32%	87.84%	89.79%
	512	60.41%	66.82%	74.72%	79.26%	77.10%	79.48%	87.41%	89.72%
SVD+whitening	256	62.29%	68.16%	71.57%	76.68%	80.74%	82.42%	85.47%	87.99%
	512	62.13%	68.13%	71.07%	76.06%	81.44%	82.82%	85.23%	87.62%

feature. In addition, VLAD and FV is employed to encode the selected deep descriptors, and we denote the two methods as “selectVLAD” and “selectFV” in Table 3. The features of selectVLAD and selectFV have longer dimensionality, but lower mAP in the retrieval task.

State-of-the-art general image retrieval approaches, e.g., SPoC and CroW, can not get satisfactory results for fine-grained images. Hence, general deep learning image retrieval methods could not be directly applied to FGIR.

We also report the results of SCDA⁺ and SCDA_flip⁺ on these four fine-grained datasets in Table 3. In general, SCDA_flip⁺ is the best among compared methods.

Post-Processing In the following, we compare several feature compression methods on the SCDA_flip⁺ feature: 1) Singular Value Decomposition (SVD); 2) Principal Component Analysis (PCA); 3) PCA whitening (whose results were much worse than other methods and are omitted) and 4) SVD whitening. We compress the SCDA_flip⁺ feature to 256-d and 512-d, respectively, and report the compressed results in Table 4. Comparing the results shown in Table 3 and Table 4, the compressed methods can reduce the dimensionality without hurting the retrieval performance. SVD (which does not remove the mean vector) has slightly higher rates than PCA (which removes the mean vector). In particular, the “256-d SVD+whitening” feature can achieve better retrieval performance (2%~3% higher) than the original SCDA_flip⁺ feature on *CUB200-2011*



Figure 7. Some retrieval results of four fine-grained datasets. On the left, there are two successful cases for each datasets; while on the right, there are failure cases. The first image in each row is the query image. Wrong retrieval results are marked by red boxes. (Best viewed in color.)

and *Oxford Flowers*. Moreover, “256-d SVD+whitening” generally achieves better performance than other compressed ones, meanwhile with less dimensions. Therefore, we take it as our optimal choice for FGIR. In the following, we present some retrieval examples based on “256-d SVD+whitening”.

In Fig. 7, we show two successful retrieval results and two failure cases for each fine-grained dataset, respectively. As shown in the successful cases, our method can work well when the same kind of birds, animals or flowers appear in different kinds of background. In addition, for these failure cases, there exist only tiny differences between the query image and the returned ones, which can not be accurately detected in this pure unsupervised setting. We can also find some interesting observations, e.g., the last failure case of the flowers and pets. For the flowers, there are two correct predictions in the top-5 returned images. Even though the flowers in the correct predictions have different colors with the query, our method can still find them. For the pets’ failure cases, the dogs in the returned images have the same pose as the query image.

4.2 Quality and Insight of the SCDA Feature

In this section, we discuss the quality of the proposed SCDA feature. After SVD and whitening, the former distributed dimensions of SCDA have more discriminative ability, i.e., directly correspond to semantic visual properties that



Figure 8. Quality demonstrations of the SCDA feature. From the top to bottom of each column, there are six returned original images in the order of one sorted dimension of “256-d SVD+whitening”. (Best viewed in color and zoomed in.)

are useful for retrieval. We use three datasets (*CUB200-2011*, *Stanford Dogs* and *Oxford Flowers*) as examples to illustrate the quality. We first select one dimension of “256-d SVD+whitening”, and then sort the value of that dimension in the descending order. Then, we visualize images in the same order, which is shown in Fig. 8.

Images of each column have some similar “attributes”, e.g., *living in water* and *opening wings* for birds; *brown and white heads* and *similar looking faces* for dogs; *similar shaped inflorescence* and *petals with tiny spots* for flowers. Obviously, the SCDA feature has the ability to describe the main objects’ attributes (even subtle ones), which might explain its success in fine-grained image retrieval. Details and more examples can be found in the supplementary material.

4.3 Classification Results

In the end, we compare with several state-of-the-art fine-grained *classification* algorithms to validate the effectiveness of SCDA from the classification perspective. In the classification experiments, we fine-tune the pre-trained VGG-16 with only the image-level labels, and add the horizontal flips of the original images as data augmentation when fine-tuning. After obtaining the fine-tuned model, we extract the $SCDA_flip^+$ as the whole image representations and feed them into a linear SVM to train a classifier. Note that, the coefficient α in classification experiments is set to 1 to let the classifier to learn and then select important dimensions automatically. The classification accuracy comparison is listed in Table 5.

The classification accuracy of our method is comparable or even better than the algorithms trained with strong supervised annotations, e.g., [4, 5]. For these algorithms using only image-level labels, our classification accuracy is compara-

Table 5. Comparison of classification accuracy on four fine-grained datasets. The “details” column is a short description of the implementation details. (“f.t.” stands for “fine-tune”, and “h.flip” is short for “horizontal flip”).

Method	Train phase		Test phase		Details	Dim.	<i>Birds</i>	<i>Dogs</i>	<i>Flowers</i>	<i>Pets</i>
	BBox	Parts	BBox	Parts						
PB R-CNN with BBox [4]	✓	✓	✓		Alex-Net; f.t. on whole images and parts; with crops	12,288	76.4%	–	–	–
Deep LAC [5]	✓	✓	✓		Alex-Net; f.t. on whole images and parts; with crops	12,288	80.3%	–	–	–
PB R-CNN [4]	✓	✓			Alex-Net; f.t. on whole images and parts; with crops	12,288	73.9%	–	–	–
Two-Level [6]					VGG-16; f.t. with part proposals	16,384	77.9%	–	–	–
Weakly supervised FG [9]					VGG-16; f.t. with h.flip	262,144	79.3%	80.4%	–	–
Constellations [7]					VGG-19; f.t. with h.flip; with part proposals	208,896	81.0%	68.6% ¹	95.3%	91.6%
Bilinear [8]					VGG-19 and VGG-M; training with h.flip	262,144	84.0%	–	–	–
Spatial Transformer Net [34]					Inception architecture; training with h.flip and crops	4,096	84.1%	–	–	–
Ours					VGG-16; f.t. with h.flip; w/o crops	4,096	80.5%	78.7%	92.1%	91.0%

¹ [7] reported the result of the *Birds* dataset using VGG-19, while the result of *Dogs* is based on the pre-trained Alex-Net model.

ble with the algorithms using similar fine-tuned strategies ([6, 7, 9]), but still has gap to those using more powerful deep architectures and more complicated data augmentations [8, 34]. The performance of ours when employing powerful deep networks, e.g., Bilinear Net [8], Spatial Transformer Networks [34] and Residual Net [35], should also increase. Because our method has less dimensions and is simple to implement, SCDA is more scalable for large-scale datasets without strong annotations and is easier to generalize. In addition, the CroW [21] paper presented the classification accuracy on *CUB200-2011* without any fine-tuning (56.5% by VGG-16). We also experiment on the 512-d SCDA feature (only contains the max-pooling part this time for fair comparison) without any fine-tuning. The classification accuracy on that dataset is 73.7%, which outperforms their performance by a large margin.

5 Conclusions

In this paper, we proposed to use solely a CNN model pre-trained on non-fine-grained tasks to the novel and difficult fine-grained image retrieval task. We proposed the Selective Convolutional Descriptor Aggregation (SCDA) method, which is unsupervised and does not require additional learning. SCDA first localized the main object in fine-grained image unsupervisedly with high accuracy. The selected (localized) deep descriptors were then aggregated using the best practices we found to produce a short feature vector for a fine-grained image. These features exhibited well-defined semantic visual attributes, which may explain why SCDA has high retrieval accuracy for fine-grained images.

In the future, we consider including the selected deep descriptors’ weights to find object parts. Another interesting direction is to explore the possibility of pre-trained models for more complicated vision tasks such as object segmentation unsupervised.

References

1. Krizhevsky, A., Sutskever, I., Hinton, G.E.: ImageNet classification with deep convolutional neural networks. In: NIPS. (2012) 1097–1105
2. Cimpoi, M., Maji, S., Vedaldi, A.: Deep filter banks for texture recognition and segmentation. In: CVPR. (2015) 3828–3836
3. Ghodrati, A., Diba, A., Pedersoli, M., Tuytelaars, T., Van Gool, L.: DeepProposal: Hunting objects by cascading deep convolutional layers. In: ICCV. (2015) 2578–2586
4. Zhang, N., Donahue, J., Girshick, R., Darrell, T.: Part-based R-CNNs for fine-grained category detection. In Fleet, D., Pajdla, T., Schiele, B., Tuytelaars, T., eds.: ECCV 2014, Part I, LNCS 8689, Springer, Switzerland (2014) 834–849
5. Lin, D., Shen, X., Lu, C., Jia, J.: Deep LAC: Deep localization, alignment and classification for fine-grained recognition. In: CVPR. (2015) 1666–1674
6. Xiao, T., Xu, Y., Yang, K., Zhang, J., Peng, Y., Zhang, Z.: The application of two-level attention models in deep convolutional neural network for fine-grained image classification. In: CVPR. (2015) 842–850
7. Simon, M., Rodner, E.: Neural activation constellations: Unsupervised part model discovery with convolutional networks. In: ICCV. (2015) 1143–1151
8. Lin, T.Y., RoyChowdhury, A., Maji, S.: Bilinear CNN models for fine-grained visual recognition. In: ICCV. (2015) 1449–1457
9. Zhang, Y., Wei, X.S., Wu, J., Cai, J., Lu, J., Nguyen, V.A., Do, M.N.: Weakly supervised fine-grained categorization with part-based image representation. IEEE Trans. Image Processing **25**(4) (2016) 1713–1725
10. Wah, C., Branson, S., Welinder, P., Perona, P., Belongie, S.: The Caltech-UCSD birds-200-2011 dataset. Tech. Report CNS-TR-2011-001 (2011)
11. Khosla, A., Jayadevaprakash, N., Yao, B., Fei-Fei, L.: Novel dataset for fine-grained image categorization. In: CVPR Fine-Grained Visual Categorization workshop. (2011) 806–813
12. Nilsson, M.E., Zisserman, A.: Automated flower classification over a large number of classes. In: Proc. Indian Conf. Computer Vision, Graphics and Image Processing. (2008) 722–729
13. Parkhi, O.M., Vedaldi, A., Zisserman, A., Jawahar, C.V.: Cats and dogs. In: CVPR. (2012) 3498–3505
14. Jégou, H., Douze, M., Schmid, C., Pérez, P.: Aggregating local descriptors into a compact image representation. In: CVPR. (2010) 3304–3311
15. Sánchez, J., Perronnin, F., Mensink, T., Verbeek, J.: Image classification with the Fisher vector: Theory and practice. Int’l J. Computer Vision **105**(3) (2013) 222–245
16. Razavian, A.S., Azizpour, H., Sullivan, J., Carlsson, S.: CNN features off-the-shelf: An astounding baseline for recognition. In: CVPR Deep Vision workshop. (2015) 806–813
17. Gong, Y., Wang, L., Guo, R., Lazebnik, S.: Multi-scale orderless pooling of deep convolutional activation features. In Fleet, D., Pajdla, T., Schiele, B., Tuytelaars, T., eds.: ECCV 2014, Part VII, LNCS 8695, Springer, Switzerland (2014) 392–407
18. Babenko, A., Slesarev, A., Chigorin, A., Lempitsky, V.: Neural codes for image retrieval. In Fleet, D., Pajdla, T., Schiele, B., Tuytelaars, T., eds.: ECCV 2014, Part I, LNCS 8689, Springer, Switzerland (2014) 584–599
19. Paulin, M., Douze, M., Harchaoui, Z., Mairal, J., Perronnin, F., Schmid, C.: Local convolutional features with unsupervised training for image retrieval. In: ICCV. (2015) 91–99

20. Babenko, A., Lempitsky, V.: Aggregating deep convolutional features for image retrieval. In: ICCV. (2015) 1269–1277
21. Kalantidis, Y., Mellina, C., Osindero, S.: Cross-dimensional weighting for aggregated deep convolutional features. arXiv:1512.04065
22. Wang, J., Song, Y., Leung, T., Rosenberg, C., Wang, J., Philbin, J., Chen, B., Wu, Y.: Learning fine-grained image similarity with deep ranking. In: CVPR. (2014) 1386–1393
23. Xie, L., Wang, J., Zhang, B., Tian, Q.: Fine-grained image search. IEEE Trans. Multimedia **17**(5) (2015) 636–647
24. Girshick, R., Donahue, J., Darrell, T., Malik, J.: Rich feature hierarchies for accurate object detection and semantic segmentation. In: CVPR. (2014) 580–587
25. Simonyan, K., Zisserman, A.: Very deep convolutional networks for large-scale image recognition. In: ICLR. (2015) 1–14
26. Hinton, G.E.: Learning distributed representations of concepts. In: Annual Conf. Cognitive Science Society. (1986) 1–12
27. Bengio, Y., Courville, A., Vincent, P.: Representation learning: A review and new perspectives. IEEE Trans. Pattern Analysis and Machine Intelligence **35**(8) (2013) 1798–1828
28. Georgopoulos, A.P., Schwartz, A.B., Kettner, R.E.: Neuronal population coding of movement direction. Science **233**(4771) (1986) 1416–1419
29. Azizpour, H., Laptev, I.: Object detection using strongly-supervised deformable part models. In Fitzgibbon, A., Lazebnik, S., Perona, P., Sato, Y., Schmid, C., eds.: ECCV 2012, Part I, LNCS 7572, Springer, Heidelberg (2012) 836–849
30. Wei, X.S., Gao, B.B., Wu, J.: Deep spatial pyramid ensemble for cultural event recognition. In: ICCV ChaLearn Looking at People workshop. (2015) 38–44
31. Hariharan, B., Arbeláez, P., Girshick, R., Malik, J.: Hypercolumns for object segmentation and fine-grained localization. In: CVPR. (2015) 447–456
32. Long, J., Shelhamer, E., Darrell, T.: Fully convolutional networks for semantic segmentation. In: CVPR. (2015) 3431–3440
33. Vedaldi, A., Lenc, K.: MatConvNet: Convolutional neural networks for MATLAB (2014) <http://www.vlfeat.org/matconvnet/>.
34. Jaderberg, M., Simonyan, K., Zisserman, A., Kavukcuoglu, K.: Spatial transformer networks. In: NIPS. (2015) 2008–2016
35. He, K., Zhang, X., Ren, S., Sun, J.: Deep residual learning for image recognition. arXiv:1512.03385